

## Localized Corrosion Resistance of Dissimilar Aluminum Alloys Joined by Friction Stir Welding (FSW)

ALINE F.S.Bugarin<sup>1, a</sup>, FERNANDA M. Queiroz<sup>2, b</sup>, MAYSA Terada<sup>2, c</sup>,  
HERCILIO G. de Melo<sup>2, d</sup> and ISOLDA Costa<sup>1, e\*</sup>

<sup>1</sup>Instituto de Pesquisas Energéticas e Nucleares, Av. Prof. Lineu Prestes, 2242, CEP 05508-000, São Paulo - SP

<sup>2</sup>Depto. de Eng. Metalúrgica e de Materiais, Universidade de São Paulo, Av. Prof. Mello Moraes, 2463, CEP 05508-030, São Paulo – SP, Brasil

<sup>a</sup>afbugarin@usp.br, <sup>b</sup>mq\_fernanda@yahoo.com.br, <sup>c</sup>maysaterada@uol.com.br <sup>d</sup>hgdemelo@usp.br, <sup>e\*</sup>icosta@ipen.br

**Keywords:** Localized corrosion, FSW, dissimilar alloys, aluminum alloys, AA2024, AA7475.

**Abstract.** 2XXX and 7XXX high strength aluminum alloys are the most used materials for structural parts of aircrafts due to their high strength/weight ratio. Their joining procedure is an engineering challenge since they present low weldability. Friction Stir Welding (FSW) is a joining technology developed in the early 90's. It is a solid-state welding process, without the use of fillers or gas shield, that eliminates conventional welding defects and has been considered of great interest for application in the aircraft industry. FSW of aluminum alloys results in four regions of different microstructures, specifically: the base material (BM), the heat affected zone (HAZ), the thermo-mechanically affected zone (TMAZ), and the nugget zone (NZ). The complex microstructure of the weld region leads to higher susceptibility to localized corrosion as compared to the BM even when similar alloys are joined. The welding of dissimilar alloys in its turn results in even more complex microstructures as materials with intrinsically different composition, microstructures and electrochemical properties are put in close contact. Despite the great interest in FSW, up to now, only few corrosion studies have been carried out for characterization of the corrosion resistance of dissimilar Al alloys welded by FSW. The aim of this study is to investigate the corrosion behavior of aluminum alloy 2024-T3 (AA2024-T3) welded to aluminum alloy 7475-T761 (AA7475-T761) by FSW. The evaluation was performed in 0.01 mol.L<sup>-1</sup> solution by means of open circuit potential measurements, polarization techniques and surface observation after corrosion tests.

### Introduction

The welding process known as Friction Stir Welding (FSW) was developed in 1991 by the “The Welding Institute (TWI)” – UK. Since then, this joining procedure has found many applications in various industries such as automotive, aerospace, marine, food and nuclear [1-3]. Conventional welding processes lead to melting of the aluminum alloys creating defects in the welded joints, such as porosities, cracks and residual stresses [3-5]. FSW process does not involve fusion, avoiding such microstructural defects and reducing residual stresses. Unlike other procedures, FSW consists in a solid state welding, where the pin of a non-consumable rotating tool penetrates between the two materials to be welded and is displaced along the joint line. High temperatures and plastic deformation guarantee welding without fusion. Another advantage of this process is that it eliminates the need for metal addition or gas shielding [3,5,6]. FSW characteristics result in increased efficiency of welded joints, being successfully used for welding high-strength aluminum alloys, such as those of the 2XXX and 7XXX series [2,7,8].

Despite its advantages, the FSW process produces a complex microstructure with the formation of distinct zones ascribed to the heat flow associated or not with mechanical deformation. Such zones are: the nugget or the mixture zone (NZ), the thermomechanically affected zone (TMAZ), the heat affected zone (HAZ), besides the base metal (BM), that is, the areas that remain unaffected by heat or thermomechanical effects related to the FSW process.

Hai-long Qin *et al.* [9] investigated the exfoliation corrosion (EXCO) behavior of the AA2A14-T6 alloy welded by FSW (FSWed) by immersion tests. The results showed that comparatively to the base metal, the exfoliation corrosion resistance of the FSW affected zone was greater; besides, the weld nugget presented the highest corrosion resistance among the affected zones. On the other hand, Astarita *et al.* investigated the stress corrosion cracking (SCC) behavior of various FSWed 2XXX series alloys and found that all the tested joints were susceptible not only to intergranular but also to pitting corrosion, and for the samples of the 2XXX series, the welded region showed an anodic behavior in comparison with the base metal[10]. The main benefits of FSW compared with conventional welding methods are the lower heat input, the low distortion of the welded material and the lack of cracks by heating. Besides, materials of various thicknesses can be joined and the process automated, ensuring fast, economic and reproducible results [1,7]. Studies have shown a great improvement in the fatigue resistance of the surface of FSWed AA8090 butt joints. The reduction of surface irregularities limited the generation of local plasticity conditions, reducing crack propagation [11]

Dissimilar materials can be easily welded for FSW. However, for this particular situation the joined materials can become very susceptible to galvanic coupling effects, increasing the susceptibility of the welding region to localized corrosion [2,6]. Sidane *et al* [8] employed local electrochemical techniques to investigate the corrosion behavior of aluminum alloys 2050-T8 and 7449-T79 joined by FSW. Their results indicated galvanic coupling effects at the interface between the alloys and the nugget zone, and different kinetics at the interfaces between the zones of diverse microstructures around the nugget. This was associated to the electric characteristics of the passive layer that were different on each one of the alloys. The results of localized electrochemical impedance spectroscopy (LEIS) experiments indicated higher current densities at the interface of the alloys or at the interface between zones with different microstructures, suggesting faster kinetics of the corrosive processes at these regions, which was ascribed to galvanic coupling [12].

Astarita *et al* [13] performed SCC tests to dissimilar FSWed alloys (AA2198 and AA6056). They studied the critical issues related to the welding of dissimilar heat treated aluminum alloys and found that the welded materials presented crevice corrosion, as well as galvanic corrosion[13].

The indication of galvanic coupling was also proposed by Jariyaboon *et al* [6]. They investigated the corrosion resistance of AA2024-T351 and AA7010-T7651 alloys joined by FSW, in NaCl 0.1 mol.L<sup>-1</sup>. They observed more severe corrosion at the central zone of the nugget, due to galvanic coupling of the anodic AA7010 alloy with the cathodic AA2024-T351 alloy, promoting strong corrosive attack between the two alloys.

Despite the great interest and increasing studies on the electrochemical behavior of dissimilar alloys joined by FSW, the published literature on this subject is still limited. The aim of the present investigation is to study the microstructure and the corrosion resistance of AA2024-T3 joined to AA7475-T761 alloy by FSW in 0.01 mol.L<sup>-1</sup> solution.

## Materials and Methods

The material of this study was supplied by Embraer as thin plates of AA2024-T3 joined to AA7475-T761 by FSW. The chemical compositions of the parent alloys are shown in Table 1. The AA2024 plate was on the advancing side of the weld, while the AA7475 plate was on the retreating side, as Fig. 1 illustrates.

Table 1 - Chemical compositions of AA2024-T3 and AA7475-T761 alloys (wt.%)\*

Alloy	Al	Mg	Si	P	S	Ca	Ti	Cr	Mn	Fe	Cu	Zn
2024	Bal.	1.6±	0.19±	0.03±	0.02±	0.04±	0.05±	0.04±	0.64±	0.22±	4.8±	0.08±
		0.2	0.02	0.01	0.01	0.01	0.01	0.02	0.06	0.01	0.5	0.01
7475	Bal.	1.9±	0,15±	0.03±	0.05±	0.06±	0.04±	0.22±	0.02±	0.12±	1,7±	6.2 ±
		0.2	0.02	0.01	0.01	0.01	0.01	0.01	0.01	0.01	0.02	0.2

\* Fluorescence Spectrometry by X-ray wavelength dispersion.

According to NBR 6835, “T3” indicates that the AA2024 was heat treated, strain hardened and naturally aged. On the other hand, “T761” means that the AA7475 was heat treated and artificially aged [14].

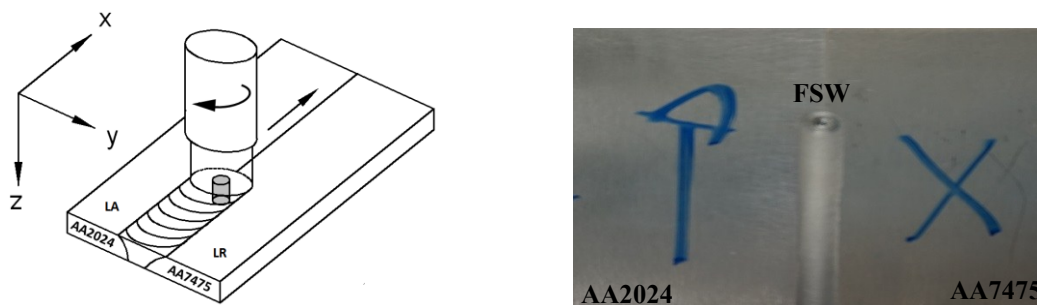


Fig. 1 – (a) Illustration of the FSW process showing the advance (LA) and the retreating (LR) sides, and the tool rotation and displacement direction, and (b) macrograph of the two alloys joined by FSW.

### Samples preparation

Before any microstructural and electrochemical analysis, samples were grinded with silicon carbide paper up to #4000, followed by polishing with diamond paste (up to 1  $\mu\text{m}$ ), degreased in ethyl alcohol, washed with deionised water and dried under hot air stream. For optical microscopy observations, the samples were further etched with a solution of 25mL  $\text{HNO}_3$  and 2mL HF in 100 mL  $\text{H}_2\text{O}$ , to preferentially reveal the grain boundaries of the alloys.

### Electrochemical tests

Open circuit potential (OCP) measurements were carried out at zones of the BM corresponding to the two alloys and at the whole FSW zone and surroundings. For these measurements, the exposed area to the 0.01 mol.L<sup>-1</sup> NaCl electrolyte corresponded to 1.0 cm<sup>2</sup>. Anodic and cathodic polarization curves were obtained for similar zones with the same exposed areas. The curves were obtained separately from freshly prepared surfaces and after OCP stabilization. For these tests a three electrodes cell set-up was used with an Ag/AgCl KCl<sub>sat</sub> and a platinum wire as reference and counter electrode, respectively. OCP measurements were also obtained with a microcell (0.038 cm<sup>2</sup>), restraining the exposed area to specific weld zones, such as the TMAZ and NZ. All experiments were carried out in aerated conditions at (22±2) °C.

### Results

Fig. 2 depicts the microstructure obtained by optical microscopy after etching of the different weld zones of the AA2024-T3 and AA7475-T761 joined by FSW. As verified by other authors [6], they show significant effects of the FSW on the alloys microstructures, such as change in grain sizes, material mixture and well defined heterogeneous interfaces, such as those found between the nugget and TMAZ, or between the TMAZ and HAZ of the two alloys. In the weld zone, the precipitates seem to be preferentially distributed along the direction of the rotating tool dragging them during its swirling movement. This is more evident at the interface between the TMAZ and the HAZ. At this latter zone, the interface between the two alloys is clearly identifiable, and shows the effect of the rotating tool on trying to mix the two alloys, generating a comb like structure. The microstructure of the two alloys in the HAZ (Fig. 2d and 2e) are similar and composed by irregular grains with different sizes, generally, in this zone, the thermal cycle is not enough to differentiate the grain size from the BM. These results suggest that the zones affected by the FSW process may present increased corrosion susceptibility due to galvanic coupling effects.

The cathodic polarization curves of all tested zones (not presented) showed diffusion controlled reduction. The anodic polarization curves of the whole FSW zone and at areas of the two BM not affected by the heat input are presented in Fig. 3. They show that, irrespectively to the configuration, the corrosion potential of the different samples are above the pitting potential and that is difficult to differentiate the anodic activity between the samples. Besides, the corrosion potential of the sample including the FSW affected zones is below the corrosion potential of the two alloys separately indicating that FSW affects the electrochemical activity of the weld zones. The heterogeneous nature of the different weld zones are evidenced in the results obtained with the microcell ( $0.038 \text{ cm}^2$ ), Fig. 4, that show strong differences between the OCP of the isolated weld zones).

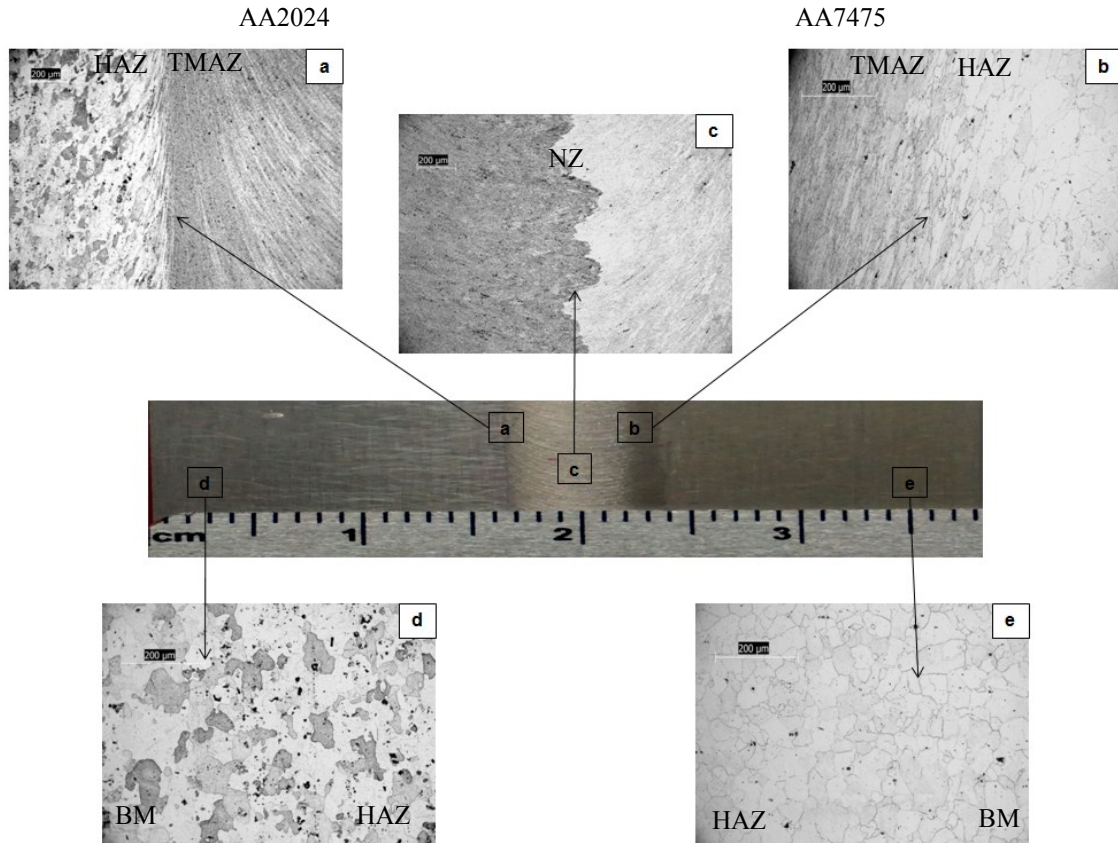


Fig. 2 – Optical micrographs of the different zones of the alloys joined by FSW, showing (a) interface between the heHAZ and the TMAZ of the AA2024 alloy, (b) interface between the HAZ and TMAZ of the AA7475 (c) Nugget (NZ), (d) BM of the AA2024 and (e) BM of the AA7475 alloy.

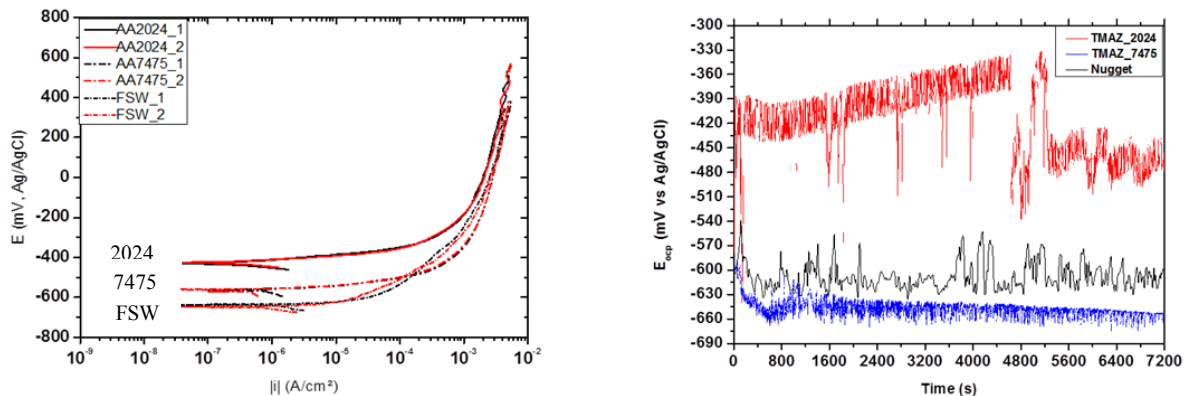


Fig. 3 – (a). Anodic polarization curves obtained for the BM of the AA2024 and AA7475 alloys and for the whole weld region and (b) OCP of TMAZ of the AA2024 and AA7475 alloys and NZ in  $0.01 \text{ mol.L}^{-1} \text{ NaCl}$  solution.

The OCP results (Fig. 4) showed that the TMAZ of both alloys are very active with large and frequent potential oscillations and that AA7475 is anodic in comparison to AA2024 (also evidenced in Fig. 3). The large potential oscillations suggest high electrochemical activities at the zones affected by FSW, whereas the potential differences between the two TMAZ point to possible galvanic coupling effects on the electrochemical activity of these zones when exposed together to aggressive electrolytes. This latter feature is expected mainly at the NZ where both alloys interfaces each other in a comb like structure (Fig. 2(c)). The results also show that the OCP measured at the NZ is close to that of the TMAZ of the AA7475 (Fig. 3(b)), suggesting an anodic control of the corrosion process at the nugget zone by the electrochemical activity at the AA7475. The results also indicated lower OCP of the TMAZ comparatively to the BM of each alloy (compare to Fig. 3(a)).

The surface of the NZ after exposure for 4h to the 0.01 mol.L<sup>-1</sup> NaCl solution showed intense attack in the AA2024 alloy (darker areas of the comb like structure), mainly at the interface between the two alloys, AA2024 and AA7475 (lighter areas), as Fig. 4 (a) shows. Considering that AA2024-T3 is clearly cathodic to AA7475-T761, it is proposed that the intense localized attack in this former alloy could be attributed to enhanced cathodic activity at noble intermetallics on the alloy microstructure. Alkalinization near these microstructural features would damage the oxide layer provoking chemical attack of the AA2024-T3 matrix.

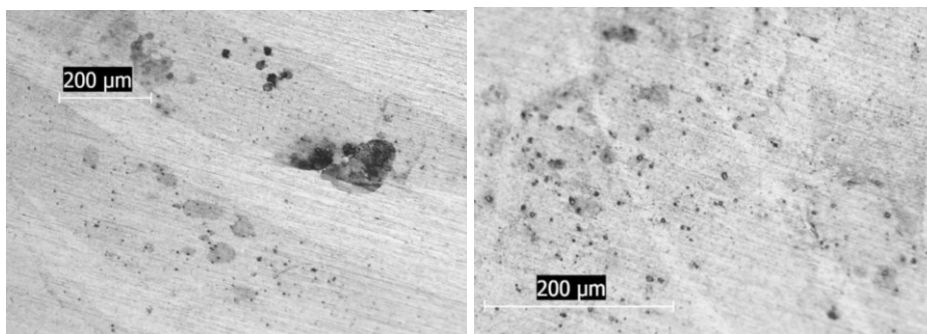


Fig. 4 – Optical micrographs of the surface of AA 2024-T3 and AA7475-T651 alloys joined by FSW showing the (a) nugget zone and (b) the TMAZ of AA2024-T3 alloy after 5 h exposure to 0.01 mol.L<sup>-1</sup> NaCl solution. In (a) darker zones are AA2024-T3 and clearer zones AA7475-T761.

## Conclusions

The results of this study indicated the effect of FSW of dissimilar aluminium alloys on their microstructure and the electrochemical activity of the various zones affected by the welding process. Galvanic coupling was suggested mainly at the nugget zone that showed a comb like structure. The effect of galvanic coupling at the nugget zone was indicated by the open circuit potentials and surface observation after corrosion immersion test. AA2024-T3 was cathodic to AA7475 and cathodic attack led to localized corrosion of the former alloy mainly at the interface with AA7475.

## Acknowledgements

The authors are grateful to CNPq for the grants to F.M. Queiroz (Processo 150847/2015-7) and to A.F.S. Bugarin, to CAPES for the grant to M.Terada (1536157), to FAPESP for financial support (Processo 2013/13235-6) and to Embraer for providing the material for study.

**References**

- [1] E.P. Alves, Joining of dissimilar materials using the friction stir welding process, Instituto Nacional de Pesquisas Espaciais, São José dos Campos, 2010, (*In Portuguese*).
- [2] A. S. Fioravanti, A. Suárez. Soldagem por FSW de ligas de alumínio alclad AA2024-T3 e AA7075-T6, Universidade Federal do Rio Grande do Sul, Porto Alegre, 2008.
- [3] P. L. Threadgill, A.J. Leonard, H.R. Shercliff, P. J. Withers, Friction stir welding of aluminium alloys, *Int. Mater. Reviews*. 54 (2009) 49-93.
- [4] G. Çam, S. Mistikoglu, Recent Developments in Friction Stir Welding of Al-alloys, *J. Mater. Eng. Perform.* 23(2014) 1936-1953.
- [5] C. Shen, J. Zhang, J. Ge, Microstructures and electrochemical behaviors of the friction stir welding dissimilar weld. *J. Environ. Sci.* (2011) 32-35.
- [6] M. Jariyaboon, J. Davenport, R. Ambat, B.J. Connolly, S.W. Williams, D.A. Price, Corrosion of a dissimilar friction stir weld joining aluminium alloys AA2024 and AA7010. *Corrosion Eng. Sci. Technol.* 41(2006) 135-142.
- [7] E.A. Marconato, Influence of defects in the mechanical properties of joints welded by FSW of the AA6013-T6, UFSCar, São Carlos, 2011, (*In Portuguese*).
- [8] D. Sidane, E. Bousquet, O. Devos, M. Puiggali, M. Touzet, V. Vivier and, A. Poulon-Quintin, Local electrochemical study of friction stir welded aluminum alloy assembly, *J. Electroanal. Chem.* 737 (2014) 206-211.
- [9] H. Qin, H. Zhang, Sun, Q. Zhuang, Corrosion behavior of the friction-stir-welded joints of 2A14-T6 aluminum alloy, *Int. J. Miner., Metall and Mater.* 22 (2015) 627-638.
- [10] A. Astarita., C. Bitondo, A. Squillace, E. Armentani, F. Bellucci, Stress corrosion cracking behaviour of conventional and innovative aluminium alloys for aeronautic applications, *Surf. Interface Anal.* 45 (2013) 1610-1618.
- [11] M. Pedemonte, C. Gambaro, E. Lertora, C. Mandolfino, Fatigue assessment of AA 8090 friction stir butt welds after surface finishing treatment, *Aerosp. Sci. Technol* 27 (2013) 188-192.
- [12] L. Lacroix, C. Blanc, N. Pébère, G.E. Thompson, B. Tribollet, V. Vivier. Simulating the galvanic coupling between S-Al<sub>2</sub>CuMg phase particles and the matrix of 2024 aerospace aluminium alloy, *Corr. Sci.* 64 (2012) 213–221.
- [13] A. Astarita, A. Squillace, A. Scala, and A. Prisco. On the Critical Technological Issues of Friction Stir Welding T-Joints of Dissimilar Aluminum Alloys. *J. Mater. Eng. Perform.* 21 (2011) 1763-1771.
- [14] ABNT. NBR 6835: Aluminium and its alloys – Classification of quenching. Rio de Janeiro: Copyright, 2000, 6 p, (*In Portuguese*).